applied mechanics

Article

Tensile Properties of 3D-Printed Jute-Reinforced Composites via Stereolithography

M. Azizur Rahman [1], Arafath Mohiv [2], M. Tauhiduzzaman [3], Md. Kharshiduzzaman [2], Md. Ershad Khan [4], Mohammad Rejaul Haque [2] and Md. Shahnewaz Bhuiyan [2,*]

1 BRAC Business School, BRAC University, Dhaka 1212, Bangladesh; azizur.rahman@bracu.ac.bd
2 Department of Mechanical and Production Engineering, Ahsanullah University of Science and Technology, Dhaka 1208, Bangladesh; arafathmohivmunna@gmail.com (A.M.); kharshid.mpe@aust.edu (M.K.); md.rejaulh37.mpe@aust.edu (M.R.H.)
3 National Research Council of Canada, 800 Collip Circle, London, ON N6G 4X8, Canada; mohammed.tauhiduzzaman@nrc-cnrc.gc.ca
4 Department of Textile Engineering, Ahsanullah University of Science and Technology, Dhaka 1208, Bangladesh; ershad.dtt@aust.edu
* Correspondence: newaz.mpe@aust.edu

Abstract: This paper investigates the tensile properties of jute-reinforced composites fabricated using stereolithography (SLA) 3D printing. Tensile tests were conducted using dog-bone tensile specimens following ASTM D638 Type IV specifications. Additionally, the study explores the effect of layer thickness on the tensile properties of the 3D-printed composite material, examining four different layer thicknesses: 0.025 mm, 0.05 mm, 0.075 mm, and 0.1 mm. The findings revealed that the tensile strength of the 3D-printed jute-reinforced composites increased with the printing layer thickness, reaching its maximum at a layer thickness of 0.1 mm. This represents an enhancement of approximately 84% compared to pure resin. Examination of the fiber–matrix interface under an optical microscope revealed a wavy pattern, suggesting that the interface may act as a mechanical interlock under tensile loads, thereby significantly enhancing tensile strength. The strength of the 3D-printed jute-reinforced composites was found to be comparable to that of glass fiber mat epoxy composites. This demonstrates that 3D SLA-printed jute-reinforced composites offer a promising avenue for producing next-generation composites that are typically challenging to manufacture using traditional fabrication techniques.

Keywords: natural fiber-reinforced composites; 3D printing; tensile properties; jute fibers

Citation: Rahman, M.A.; Mohiv, A.; Tauhiduzzaman, M.; Kharshiduzzaman, M.; Khan, M.E.; Haque, M.R.; Bhuiyan, M.S. Tensile Properties of 3D-Printed Jute-Reinforced Composites via Stereolithography. *Appl. Mech.* **2024**, *5*, 773–785. https://doi.org/10.3390/applmech5040043

Received: 4 August 2024
Revised: 25 October 2024
Accepted: 28 October 2024
Published: 31 October 2024

1. Introduction

The transportation sector, particularly the automobile sector, accounts for approximately 75% of all carbon emissions, contributing nearly 6 gigatons of CO_2 annually [1]. Consequently, manufacturers and consumers are increasingly adopting "cradle-to-beyond-the-grave" approaches in product design, prioritizing materials that are both renewable and environmentally benign [2]. In this regard, plant-based natural fiber-reinforced composites can be used for an attractive research area in composite manufacturing due to their low cost, low energy consumption, low density, and light weight. They also offer acceptable specific strength properties, recyclability, enhanced thermal properties, and a reduction in air pollution [3–5]. A wide range of lignocellulose fibers, including cotton, jute, flax, bamboo, sisal, hemp, kenaf, rice husk, ramie, abaca, sugarcane bagasse, and coconut coir [6–8], was used as reinforcers or filler for making eco-friendly composites with acceptable mechanical properties.

Jute, abundantly available in Bangladesh, is recognized for its high tensile strength, low thermal and electrical insulation properties, complete biodegradability, environmental

friendliness, good dimensional stability, and cost-effectiveness [9,10]. It primarily comprises cellulose (45–71.5%), hemicelluloses (13.6–21%), and lignin (12–26%) [11]. The high cellulose content in jute contributes to the development of strong and rigid composites when reinforced with bioresins or thermoplastic/thermoset resins. Therefore, a renewed research interest has been observed in the scientific literature on jute-reinforced composite materials. In Bangladesh, two main varieties of jute, CORCHORUS OLITORIUS (Tossa jute) and CAPSULARIS (white jute), are widely cultivated. Tossa jute, grown in highland areas, exhibits superior bundle strength compared to white jute, making it more suitable for producing stronger and more durable jute products. For our study, Tossa jute fibers were sourced from local farmers, with the fibers having an approximate height of 12–15 feet and a diameter ranging from 39 to 66 µm [12]. Numerous studies have been carried out to investigate the suitability of jute fibers for use as reinforcing components [13]. As shown in Figure 1, this study can be broadly categorized into four areas: matrix selection, surface treatments, composite fabrication methods, and the ways in which these elements influence mechanical properties. Furthermore, as depicted in Figure 1, the mechanical properties, such as tensile strength, flexure strength, impact strength, etc., of jute fiber-reinforced composite are mainly affected by numerous factors such as surface modification methods, matrix combination, and composite fabrication methods (indicated by arrows in Figure 1) [13].

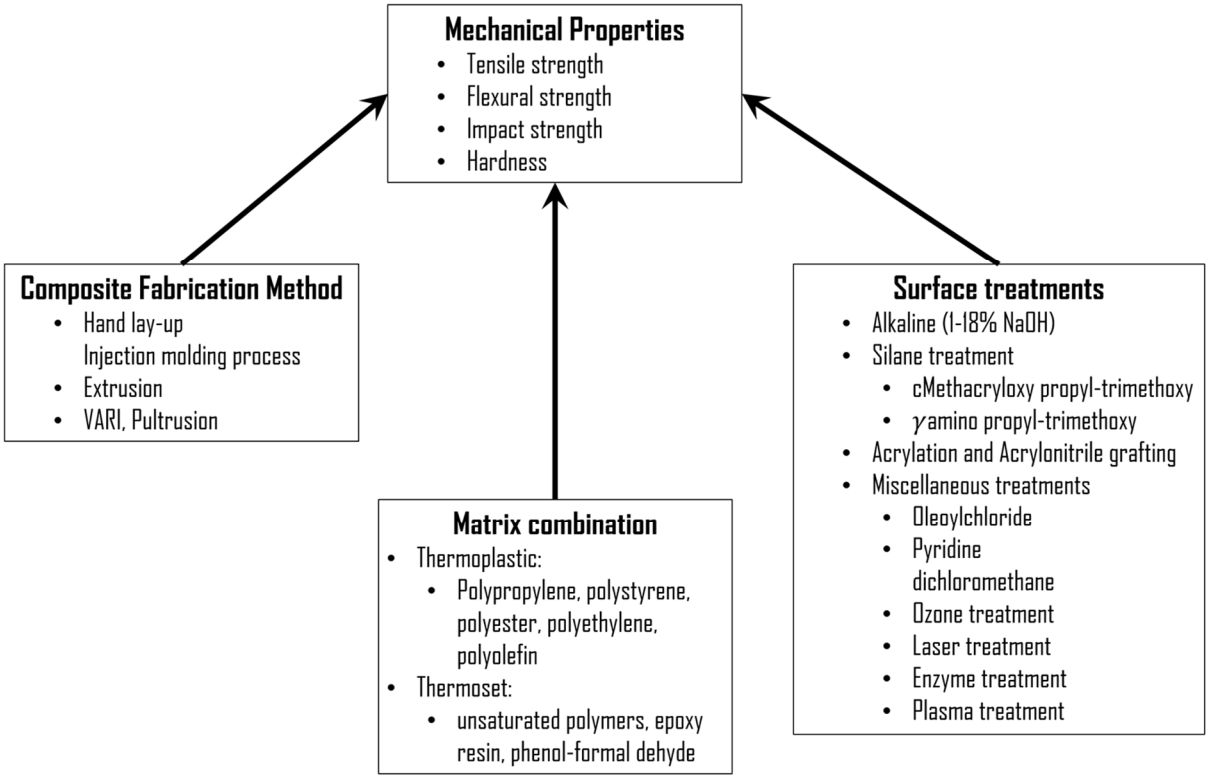

Figure 1. Summary of research categories and influencing factors for jute fiber-reinforced composites, created based on data presented in Ref. [13]. This figure is an original illustration derived from Ref. [13]'s information, not directly reproduced.

Jute-reinforced polymer composites are typically produced using traditional manufacturing methods designed for conventional fiber-reinforced polymer composites and thermoplastics. These methods include hand lay-up, injection molding, extrusion, pultrusion, and vacuum-assisted resin infusion (VARI) [13]. Despite advancements in these techniques, completely eliminating voids in fiber-reinforced composites remains nearly impossible, as void formation is inevitable and varies with the manufacturing process. N.Z.M. Zuhudi et al. [14] reported that void content can range from as low as 2% in resin

transfer molding to as high as 30% in hand lay-up with compression molding. These voids act as stress concentrators, promoting crack propagation, weakening the fiber–matrix bond, and ultimately reducing the mechanical properties of the composites.

The emergence of 3D printing, particularly in additive manufacturing, addresses many limitations of traditional techniques by allowing precise control over material deposition, which significantly reduces the likelihood of void formation. This method ensures consistent resin distribution, minimizes air entrapment, and allows for better control of the processing environment, mitigating issues like moisture absorption and wax evaporation. As a result, 3D printing can greatly reduce void content, strengthen the fiber–matrix bond, and improve the overall mechanical properties of fiber-reinforced composites.

Among various 3D printing technologies, a few technologies that are generally used in manufacturing natural fiber-reinforced composites are (i) fused deposition modeling (FDM), where material composed of natural fiber-reinforced composite filament is deposited layer by layer to form a 3D object, and (ii) stereolithography (SLA), where an ultraviolet projector is used to harden a photosensitive resin layer by layer to form a 3D object [15]. FDM-based 3D printing is the most popular and widely used additive manufacturing technology, with thermoplastic materials that have melting points below 300 °C [15], since the FDM printing temperature is around 300 °C [16]. Among the various thermoplastic materials, acrylonitrile butadiene styrene (ABS) and polylactide acid (PLA) are the most widely used ones with natural fiber fillers. However, the application of additive manufacturing technologies for processing natural fiber-reinforced composites remains limited. E. A. Franco-Urquiza et al. [17] utilized PLA-fused filament on jute fabric, demonstrating that jute fabrics have promising potential as a reinforcement material. Hinchcliffe et al. [18] attempted to fabricate continuous jute and flax fiber-reinforced PLA composites and reported that pre-stressing the continuous fiber can enhance tensile strength and flexural properties. R. Matsuzaki et al. [19] used continuous jute fibers to reinforce a PLA matrix using the fused filament fabrication (FFF) method. Their findings revealed that the composites exhibited approximately 134% higher tensile strength and a 157% higher modulus compared to pure PLA.

The literature review suggested that FDM-based printing raised some unusual issues: (i) the melting temperature of the thermoplastic is the prime parameter for choosing a suitable thermoplastic since the lignocellulose in natural fiber undergoes degradation at temperatures above 200 °C [20]; (ii) to avoid the hydrolysis of polymeric matrices as well as the nucleation and growth of water vapor during mixing, natural fiber should be dried properly [21]. An inhomogeneous mixture of filler and polymer matrix [22], accurate and precise control of temperature [23], and nucleation of voids during the manufacturing processes [24] are some listed challenges faced by FDM printing technology. Eventually, these constraints resulted in nozzle clogging in a 3D printer and inconsistent and variable mechanical properties with low fabrication accuracy. To partially circumvent these problems, SLA 3D printing has gained attention.

High resolution, good accuracy, and rapid printing times [25] make the SLA 3D printing process a powerful and versatile technique in contrast to FDM printing. In SLA, since the resin is hardened using an ultraviolet laser, the degradation of lignocellulose in natural fiber is virtually absent. Y Sano et al. [25] applied SLA 3D printing to fabricate fiber-reinforced composites and reported that the tensile strength is increased by 7.2 times more than the specimen made only of resin. S Zang applied SLA 3D printing to fabricate lignin-reinforced composites and found that composites prepared by the addition of lignin showed improved tensile strength by 46–64% [26]. However, studies related to SLA-printed composites are rare. To date, only a limited amount of research has been conducted to study the mechanical characteristics of SLA-printed nonwoven fiber-reinforced composites [26,27].

This study aims to benchmark the tensile characteristics of jute fiber-reinforced composites made by stereolithography 3D printing. The article also aims to determine the effect of printing layer thickness on the tensile properties of jute fiber-reinforced 3D-printed composites.

2. Materials and Experimental Procedures

2.1. Jute Fiber

The collected fibers were first thoroughly washed in running tap water three times and then sun-dried for 72 h. This sun-drying process took place over 12 days, with 6 h of drying each day to ensure maximum sun exposure. Afterward, the jute fibers were dried on a 3D printer's heated bed for 6 h at 100 to 105 °C, with a heating rate of 3 °C per minute, and then air-cooled to room temperature. The dried fibers were then alkali-treated by soaking them in a 1 wt. % NaOH solution for 3 h at room temperature, maintaining a 1:20 ratio. Following the alkali treatment, the fibers were thoroughly rinsed in running water to remove any residual NaOH from the surface. The fibers were then sun-dried for 72 h and subsequently dried again on the 3D printer's heated bed at 100 to 105 °C, followed by air cooling to room temperature, as shown schematically in Figure 2.

The first step or initial sun-drying phase allows a gradual reduction in moisture in the jute fibers. The second step or controlled drying phase using the heated bed of the 3D printer ensured the complete removal of any residual moisture.

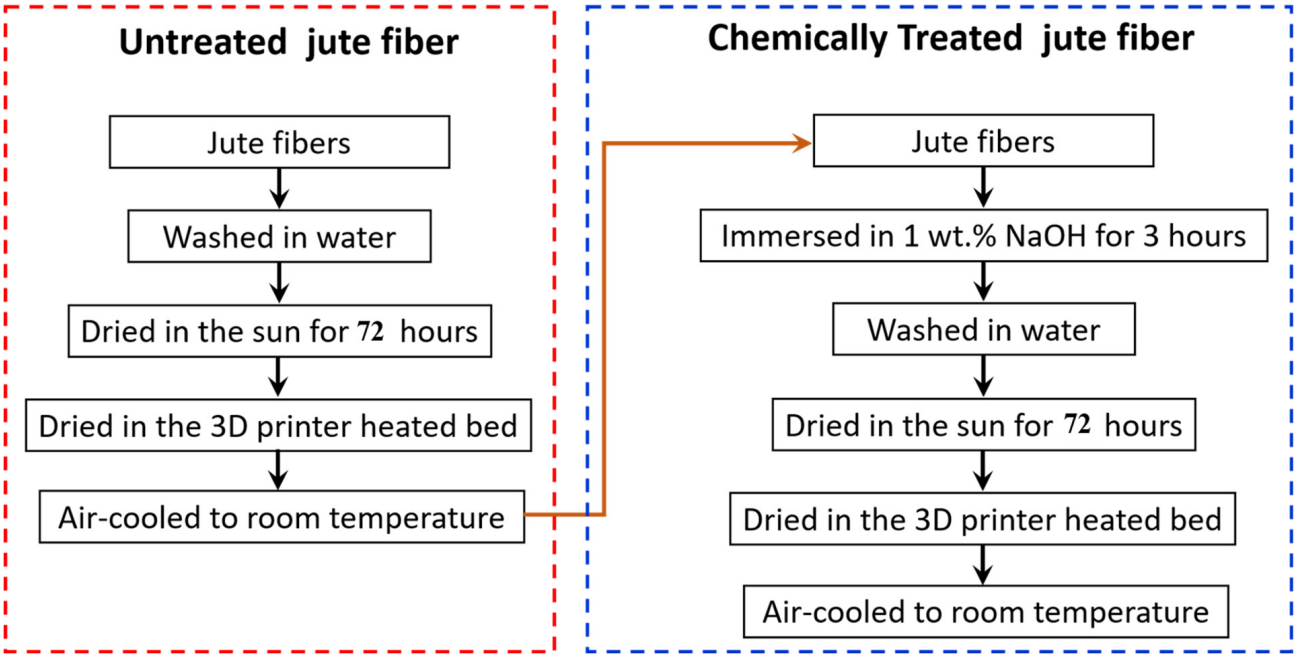

Figure 2. Schematic diagram of untreated jute fiber surface modification process.

2.2. Composite Fabrication Method

Specimens for the present study were fabricated using ANYCUBIC Photon M3 Max 3D printer machine (Shenzhen, China) with a z-axis accuracy of 0.01 mm. The machine can produce layers with thicknesses ranging from 0.01 to 0.15 mm. The geometry created in Solidworks was converted to .STL (Standard Tessellation Language) format, followed by slicing the layer using ANYCUBIC Photon Slicer software (version 3.3). The resin was cured by controlling a laser point with a wavelength of 405 nm based on the slice data. The ANYCUBIC Photon Slier software sets and manages key parameters.

A UV-curable standard photopolymer resin from Sonlu China was used as a matrix. The viscosity and density of the resin at 25 °C were 100–300 cps and 1.05–1.15 g/m^3, respectively. The curing wavelength of the resin was 405 nm.

Tensile specimens in accordance with the ASTM D638 Type IV standard (33 mm gauge length, 6 mm gauge width, and 4 mm thickness) were first designed in Solidworks. An STL (Stereolithography Interface Format) file of the tensile test specimen was then loaded into the Anycubic Photon 3D Slicer Software in order to generate G code. In the present study, printing layer thicknesses of 0.025 mm, 0.05 mm, 0.075 mm, and 0.1 mm were chosen to

understand the effect of printing layer thickness on the tensile strength of 3D-printed jute-reinforced composite. The ANYCUBIC 3D printer subsequently interpreted the generated G code to create the desired part via layer-by-layer photocuring. After printing 50% of each specimen, the 3D printer was paused to manually place the jute fibers. To ensure uniformity, the jute fibers were first weighed using a digital scale of resolution 0.001 gm. Approximately 0.2 gm of jute fibers was weighed for each sample. The weighed fibers were then combed and aligned before being positioned across the specimen. The 3D printing process then resumed to complete the fabrication of the tensile specimens. Once the printing was complete, the specimens were removed from the build plate manually and soaked in an isopropyl alcohol bath to remove un-polymerized resin on the outer surface. The printed samples were then cured using UV light for 15 min. The fabrication process of 3D-printed jute fiber-reinforced composite is depicted in Figure 3.

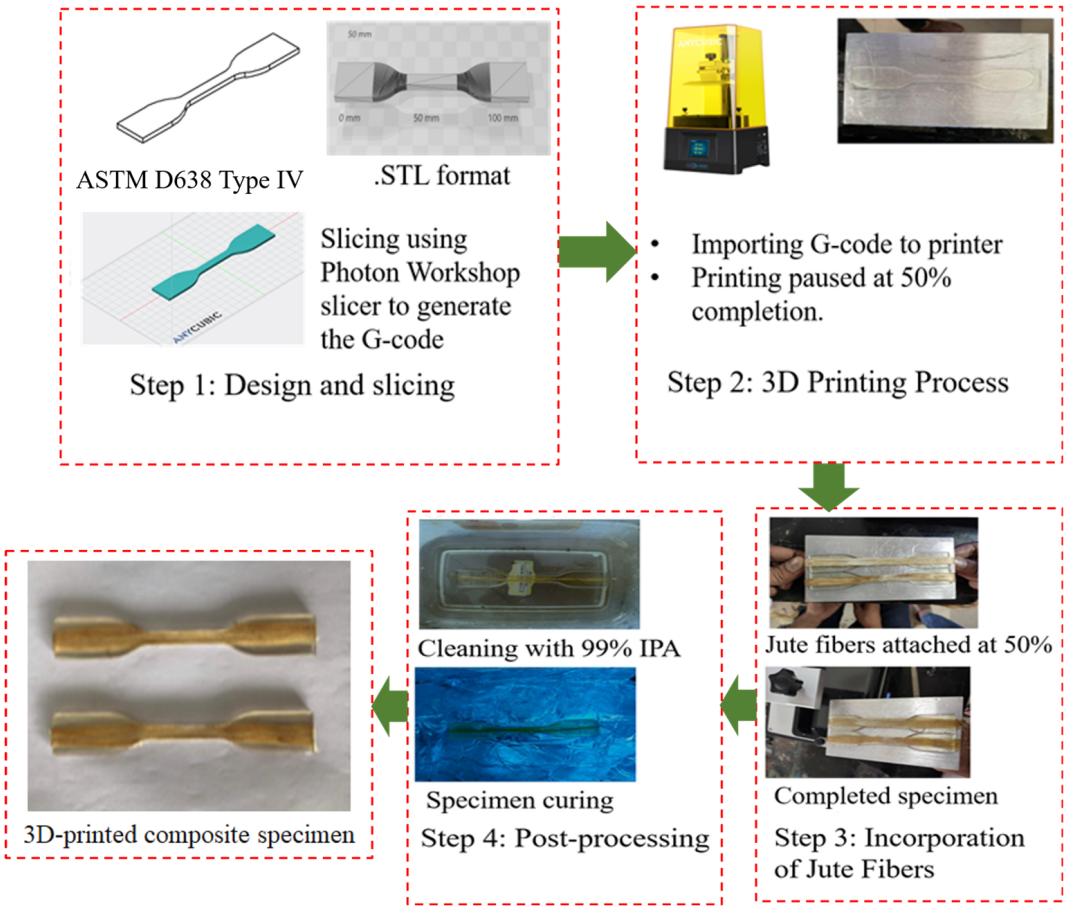

Figure 3. 3D jute fiber-reinforced composite fabrication process.

2.3. Tensile Testing

During tensile testing, it is assumed that the stresses are evenly distributed across the specimen's cross-section, reflecting the average properties throughout the material's thickness. This makes it suitable for evaluating a specific application. In contrast, stresses in flexural testing range from zero at the neutral axis to a maximum at the top and bottom surfaces, highlighting the significant influence of the specimen's properties near these surfaces. In this study, since a single layer of jute fiber was placed at the center of the specimen during the composite fabrication process, only the tensile behavior of the 3D-printed jute-reinforced composite materials was investigated.

The uniaxial tensile tests were performed on a Titan Universal Tensile Testing Machine with a 5 kN load cell. The test was carried out at about 25 °C, and the specimens were tested in tension until failure. Tensile tests were conducted with a crosshead speed of 5 mm/min and a built-in digital acquisition hardware and software system, and the machine was used to capture the force vs. extension data during the tensile tests. Up to five specimens were tested from each case, and the mean strength of the composite was calculated from the data.

2.4. FTIR Spectroscopy

The Agilent Cary 630 spectrometer (Agilent Technologies, Inc., Santa Clara, CA, USA) was used to acquire FTIR spectra for a 3D-printed UV-cured resin material, utilizing the attenuated total reflectance (ATR) mode. The measurement was conducted from 500 cm^{-1} to 4000 cm^{-1} wave number, at a resolution of 8 cm^{-1}, and involved 32 scans.

2.5. Optical Microscopy

A Motic AE2000 microscope (Motic microscopes, Hongkong, China) equipped with Motic Image Plus 3.0 software was used to observe the interface of the UV resin and jute fiber.

3. Results

3.1. FTIR Spectra of 3D-Printed Resin Material

Figure 4 depicts the FTIR spectra of the 3D-printed resin sample produced through 3D printing. Examination of Figure 4 reveals the presence of an absorption band at 3394 cm^{-1} in the high wave number region, associated with the O-H stretching mode of hydroxyl groups [28], indicating the presence of higher-molecular-weight species resulting from the ring-opening reaction of the epoxy resin. It is known that hydroxyl groups are essential for the resin's adhesion properties, which could potentially improve its bonding with natural fibers in composite applications [29]. The C-H stretching vibrations were observed at 2965, 2923, and 2863 cm^{-1} [28,30]; these peaks typically contribute to the hydrophobic character of the material, which is essential for moisture resistance in particular applications. Absorption peaks at 1724 cm^{-1} and 1635 cm^{-1} correspond to C=C stretching vibrations of aromatic rings [28], which are characteristic of the epoxy resin and exhibit very strong absorption. The resin's thermal stability and mechanical strength may be enhanced by the stability provided by these aromatic rings [31]. The absorption peak centered at 1539 cm^{-1} corresponds to C-C stretching vibrations [28]. The absorption peak at 1445 cm^{-1} was attributed to CH_3 asymmetrical bending [32], suggesting the presence of methyl groups, which may influence the cross-linking density within the resin. A higher cross-linking density typically leads to improved mechanical properties, such as tensile strength and hardness. Moreover, absorption bands related to C-O-C and C-O stretching vibrations, indicative of ether linkages, were observed at 1239, 1162, and 1029 cm^{-1} [28,30]. These functional groups indicate that the resin may provide an optimal mix of rigidity and flexibility, making it well suited for a range of engineering applications. Thus, FTIR spectroscopy confirms that the 3D-printed resin material has undergone extensive curing, resulting in a highly cross-linked network after the curing process. These findings are consistent with other studies in the literature, reinforcing the resin's suitability for advanced manufacturing applications.

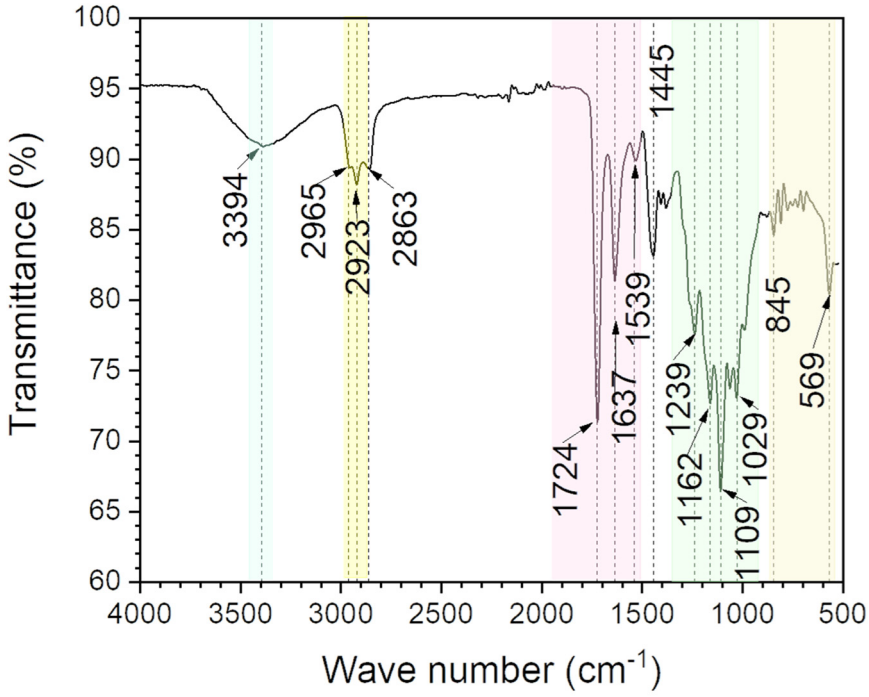

Figure 4. FTIR spectra of the 3D-printed resin sample.

3.2. Tensile Tests of 3D-Printed Resin and the Jute Fiber-Reinforced Composites

Figure 5 shows the typical force versus displacement curves for the 3D-printed standard resin. The maximum load, corresponding to the ultimate tensile strength was observed just before the failure of the specimen. The average tensile strength of the 3D-printed resin is tabulated in Table 1. Note that the ultimate tensile strength of both the 3D-printed resin and 3D-printed jute-reinforced composite material with a printing layer thickness of 0.1 mm are shown for comparison. It can be seen from Table 1 that the 3D-printed resin samples showed an average ultimate tensile strength of 20.4 MPa with a standard deviation of 1.7 MPa. The 3D-printed jute-reinforced composite material showed a notable increase in tensile strength. The 3D-printed jute-reinforced composite materials with a printing layer thickness of 0.1 mm showed an average tensile strength of 37.6 MPa with a standard deviation of 4.7 MPa.

Table 1. Results of the tensile tests: average values and standard deviations based on the five samples for each material obtained from Figure 5a.

Material	Printing Layer Thickness (mm)	Ultimate Tensile Strength (MPa)	% Improvement
Resin	0.10	20.4 ± 1.7	-
3D-printed jute-reinforced composite	0.025	34.8 ± 3.7	70.6%
	0.05	35.8 ± 2.95	75.5%
	0.075	37.2 ± 3.5	82.4%
	0.10	37.6 ± 3.9	84.4%

The effect of the addition of jute as filler material on the tensile strength was evaluated using the "improvement rate", which is defined as

$$\%Improvement\ rate = \frac{\sigma_{UTS,C} - \sigma_{UTS,R}}{\sigma_{UTS,R}} \times 100 \quad (1)$$

where $\sigma_{UTS,C}$ is the ultimate tensile strength of the 3D-printed jute-reinforced composite, and $\sigma_{UTS,R}$ is the ultimate tensile strength of the resin material.

As can be seen from Table 1, with the addition of 1.8% jute as reinforced material with 0.1 mm printing layer deposition, about 84% improvement in tensile strength is achieved.

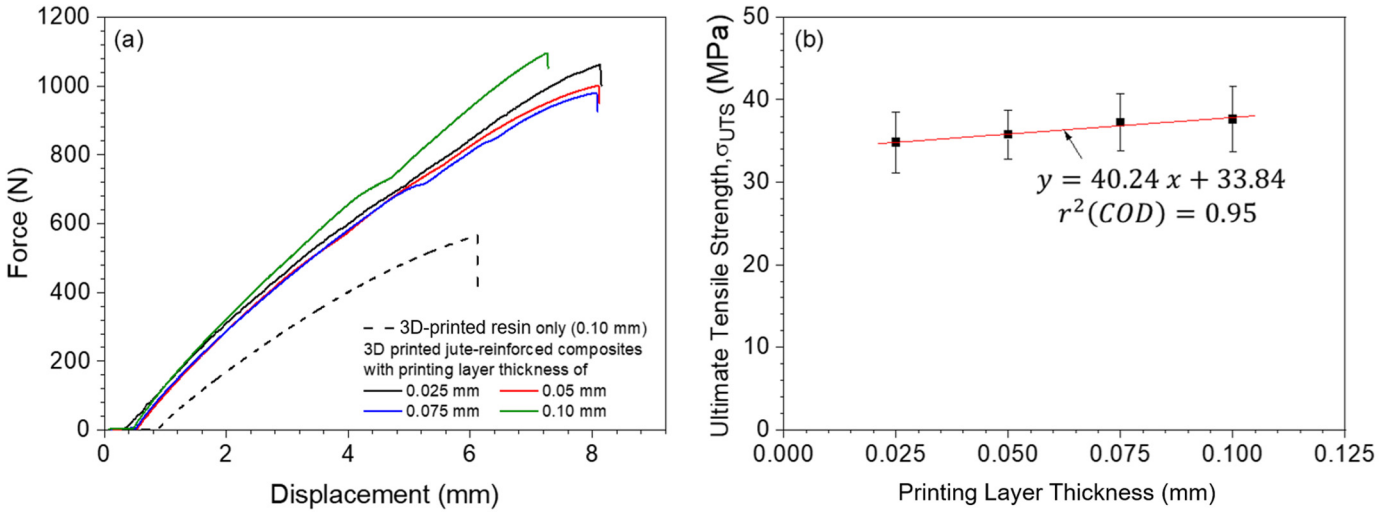

Figure 5. (**a**) Force versus displacement curve for different printing layer thicknesses. (**b**) Effect of printing layer thickness on ultimate tensile strength. For comparison, the force versus displacement curve of standard 3D-printed UV resin with 0.1 mm printing layer thickness is also shown in (**a**).

3.3. Effect of Printing Layer Thickness on Tensile Strength

The effect of printing layer thickness on the tensile strength of the 3D-printed jute-reinforced composites was investigated by employing four different printing layer thicknesses: 0.025 mm, 0.05 mm, 0.075 mm, and 0.1 mm. A typical force versus extension curve at four different deposition layer thicknesses is also shown in Figure 5a. The ultimate tensile strengths for different printing layer thicknesses are listed in Table 1 and also illustrated in Figure 5b. The results of the tensile tests, based on five specimens for each material, showed that the tensile strength of the 3D-printed jute-reinforced composites increases linearly with increasing printing layer thickness. The average ultimate tensile strength of the specimens with a 0.1 mm printing layer thickness was around 8% higher than that of the 0.025 mm specimens (Table 1).

The interface of the UV resin and jute fiber was observed under an optical microscope, and the results are shown in Figure 6. The wavy interface between the resin and jute fiber was observed. The interface was free from voids or other inclusions. As documented in Section 2.1, the dried jute fibers were alkali-treated with a 1% NaOH solution for 3 h before composite fabrication. Jute fibers, like other plant-based natural fibers, contain cellulose, hemicellulose, lignin, and wax, which smooth the fiber surface and reduce interlocking potential. However, the alkali treatment dissolves part of the lignin and hemicellulose, roughening the fiber surface [33]. This enhanced the mechanical interlocking between the fiber and matrix, leading to the formation of the observed wavy pattern at the fiber–matrix interface.

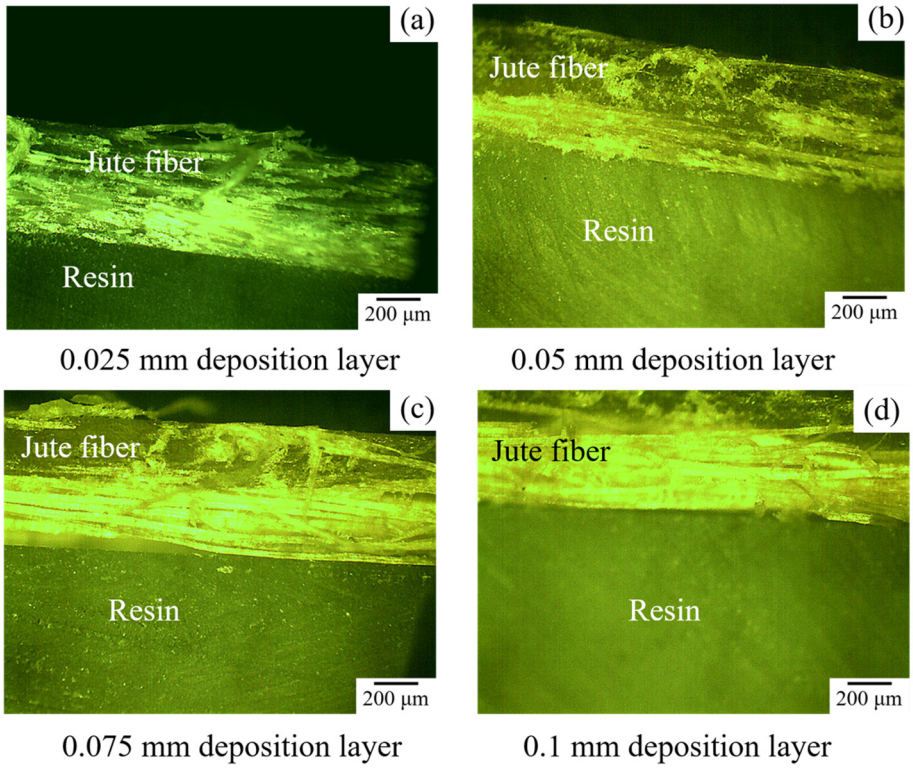

Figure 6. Optical images of 3D-printed jute fiber-reinforced composite along the fiber direction.

3.4. Comparative Study with the Literature

3.4.1. Comparison with Conventional Jute Fiber-Reinforced Composite Fabrication Method

The ultimate tensile strength of jute-reinforced composite material fabricated by conventional composite fabrication processes such as injection molding, compression molding, extrusion, and hand lay-up is compared with the present study and is shown in Figure 7a [33–39]. Most of the work reported in Figure 7a demonstrated that a large volume fraction (approximately 12% to 50%) of jute fiber is required to obtain only 50 to 85 MPa. However, this study revealed that the ultimate tensile strength of 3D-printed jute-reinforced composite is about 37.6 MPa. The 3D-printed jute-reinforced composites showed superior tensile strength compared with materials fabricated by conventional methods. Since the volume fraction of jute fiber in the 3D-printed composite used in the present study is low, raising the volume fraction can increase the ultimate tensile strength while also enhancing the performance of the composites.

3.4.2. Comparison with 3D-Printed Nonwoven Mats

Keralekas et al. [27] used one layer of commercially available nonwoven fiber mats (glass fiber, carbon, and aramid) to fabricate 3D-printed composites via stereolithography and examined the 3D-printed composites' mechanical characteristics. Later, Sano et al. [25] examined the tensile properties of 3D-printed glass fiber mat epoxy composites. In this case, they used five layers of glass fiber mats. A comparison of the ultimate tensile strength as documented by Keralekas et al. [27] and Sano et al. [25] with the present study is also shown in Figure 7b. As can be observed from Figure 7b, the ultimate tensile strength of the SLA-printed glass fiber mat–epoxy composite and carbon mat–epoxy composite is around 1.2 times higher than that obtained in the present study, whereas the five-layer glass fiber mat–epoxy composite showed around 2.1 times higher tensile strength [25]. This suggests that 3D-printed natural fiber-reinforced composites could serve as a complementary alternative to conventional composite manufacturing.

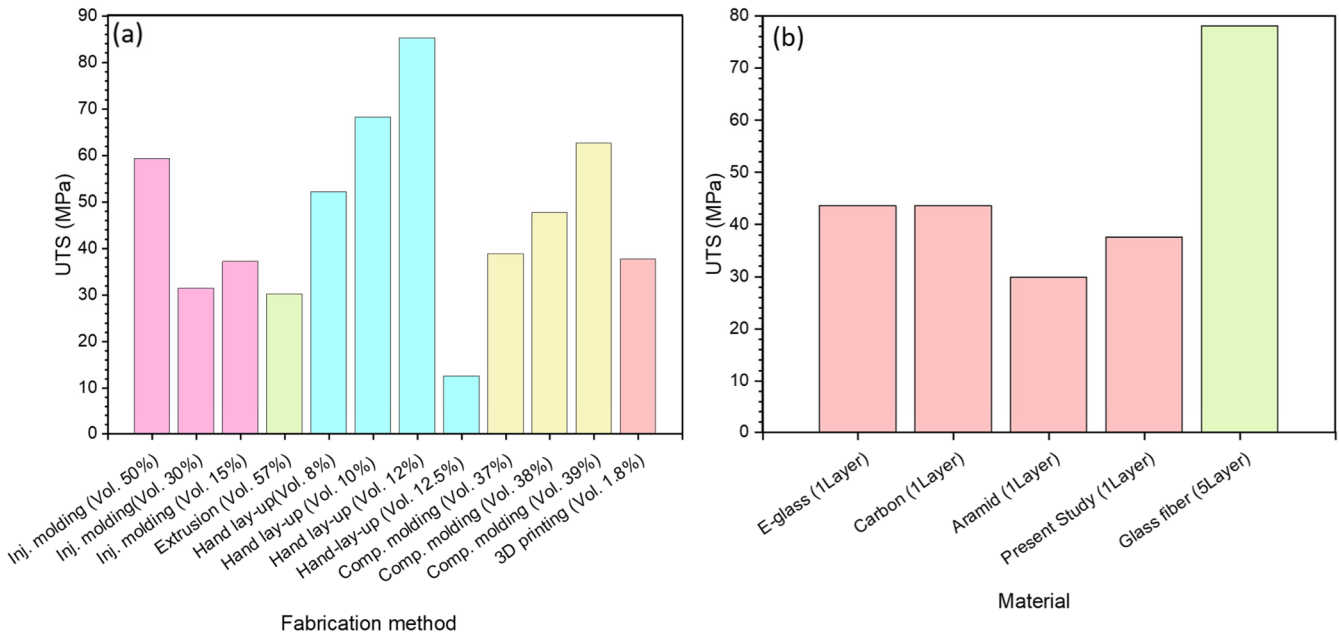

Figure 7. Comparison of ultimate tensile strength of 3D-printed jute-reinforced composites with conventional composite fabrication processes (**a**) and with 3D-printed nonwoven mats (**b**). Data were obtained from literature sources, specifically from Refs. [33–39].

4. Discussion

The results revealed a significant improvement in the tensile strength of jute-reinforced 3D-printed composite material. From the experimental results shown in Figure 5 and presented in Table 1, the tensile strength of the 3D-printed composite is increased by 84.4% compared to the similar characteristics recorded for the specimens made of pure resin. The elimination of non-cellulose substances, including hemicellulose lignin, and pectin from the interfebrile region as a result of the alkali treatments is known to increase the percentage of cellulose, which is the primary source of the enhanced strength [38]. This can be evidenced by Figure 6 where the interface between the resin and the embedded treated jute fiber is observed to be wavy. This wavy interface acts like a mechanical interlocking under tensile loads, resulting in significant improvement in the ultimate tensile strength of the 3D-printed jute-reinforced composite material [40]. These results concur with research that has been published in the literature. Rahman et al. [39] documented that the ultimate tensile strength of jute-reinforced composite increased by approximately 14–20%.

Several researchers reported that process parameters, such as layer thickness, printing orientation, post-curing time, etc., affect the mechanical properties of SLA-manufactured parts [41–43]. According to Dizon et al. [44], printing orientation has less impact on part strength than layer thickness and post-curing time. From the experimental results shown in Figure 5 and tabulated in Table 1, the average ultimate tensile strength improved with the increase of printing layer thickness, and the best result was achieved with a 0.1 mm printing layer thickness. K Chockalingam et al. [43] reported that the optimal combinations of process parameters are 0.1 mm layer thickness, which is in agreement with our study. However, the study highlights significant unexplored areas concerning the mechanical performance of jute-reinforced 3D-printed composite materials, particularly regarding the effects of post-curing time and the volume fraction of jute fibers. Future research should focus on these factors to better understand their influence on mechanical properties. Additionally, while this study primarily examined only the tensile strength, further mechanical tests, such as three-point bending, fracture toughness, impact tests, moisture absorption tests, and fiber pullout tests, are required to comprehensively characterize the 3D-printed jute-reinforced composites.

Due to economic and environmental concerns, research interest in natural fiber-reinforced composites has increased over the past 20 years. The development of these composites is still in its early stages in terms of technological maturity and fundamental understanding. Conventional processing techniques such as hand lay-up, resin transfer molding, hot press compression, and injection molding significantly impact the tensile properties of natural fiber-reinforced composite material. The advent of additive manufacturing represents a great opportunity to develop the next-generation standard composite with its synthetic equivalents (Figure 7). In conclusion, the potential for utilizing fibers in additive manufacturing remains largely untapped, but unlocking this potential could greatly enhance both the technology and the materials used. For instance, the incorporation of robotic additive manufacturing could allow for seamless fiber integration, resulting in higher-quality parts and increased productivity. Advancements in vision systems also present opportunities to develop integrated systems, enabling robots to adjust their operations in real time based on environmental changes. Moreover, the integration of artificial intelligence into robotic systems can pave the way for smart manufacturing processes, optimizing production and yielding parts with improved properties.

5. Conclusions

In this paper, the tensile properties of jute-reinforced 3D-printed composite via stereolithography have been investigated. Based on this study, the following conclusions have been reached:

- The tensile strength of 3D SLA-printed jute-reinforced composite demonstrated significant improvement in ultimate tensile strength, with an enhancement of approximately 84% compared to pure resin.
- The average ultimate tensile strength rises as the printing layer thickness increases, with the maximum strength observed at a printing layer thickness of 0.1 mm.
- Optical examination of the fiber–matrix interface revealed a wavy pattern. This wavy interface acts as a mechanical interlock under tensile loads, thereby leading to a significant enhancement in the ultimate tensile strength of the 3D-printed jute-reinforced composite material.
- The strength of the composites examined in this study was found to be comparable to that of glass fiber mat–epoxy composites. This demonstrates that SLA-printed jute fiber-reinforced composites can broaden the application of 3D printing to manufacture load-bearing components that are typically challenging to produce using traditional composite fabrication techniques.

Author Contributions: Conceptualization, M.S.B. and M.A.R.; methodology, M.S.B. and A.M.; formal analysis, A.M., M.S.B. and M.K.; investigation, M.S.B., A.M. and M.E.K.; writing—original draft preparation, M.S.B. and M.A.R., writing—review and editing, M.R.H. and M.T.; supervision, M.S.B.; project administration, M.S.B.; funding acquisition, M.S.B. and M.K. All authors have read and agreed to the published version of the manuscript.

Funding: We would like to thank the Ahsanullah University of Science and Technology (AUST) for providing a research grant (Project ID: ARP/2022/MPE/03/08) that has made this work possible.

Institutional Review Board Statement: Not applicable.

Informed Consent Statement: Not applicable.

Data Availability Statement: All data are included in the manuscript.

Conflicts of Interest: The authors declare no conflicts of interest.

References

1. Liu, Y.; Wang, Y.; Lyu, P.; Hu, S.; Yang, L.; Gao, G. Rethinking the carbon dioxide emissions of road sector: Integrating advanced vehicle technologies and construction supply chains mitigation options under decarbonization plans. *J. Clean. Prod.* **2021**, *321*, 128769. [CrossRef]

2. Chard, J.M.; Basson, L.; Creech, G.; Jesson, D.A.; Smith, P.A. Shades of Green: Life Cycle Assessment of a Urethane Methacrylate/Unsaturated Polyester Resin System for Composite Materials. *Sustainability* **2019**, *11*, 1001. [CrossRef]
3. Kumar, A.; Jyske, T.; Möttönen, V. Properties of injection molded biocomposites reinforced with wood particles of short-rotation aspen and willow. *Polymers* **2020**, *12*, 257. [CrossRef] [PubMed]
4. Righetti, M.C.; Cinelli, P.; Mallegni, N.; Massa, C.A.; Aliotta, L.; Lazzeri, A. Thermal, mechanical, viscoelastic and morphological properties of poly(lactic acid) based biocomposites with potato pulp powder treated with waxes. *Materials* **2019**, *12*, 990. [CrossRef]
5. Girometta, C.; Picco, A.M.; Baiguera, R.M.; Dondi, D.; Babbini, S.; Cartabia, M.; Pellegrini, M.; Savino, E. Physico-mechanical and thermodynamic properties of mycelium-based biocomposites: A review. *Sustainability* **2019**, *11*, 281. [CrossRef]
6. Binoj, J.S.; Raj, R.E.; Hassan, S.A.; Mariatti, M.; Siengchin, S.; Sanjay, M.R. Characterization of discarded fruit waste as substitute for harmful synthetic fiber-reinforced polymer composites. *J. Mater. Sci.* **2020**, *55*, 8513–8525. [CrossRef]
7. Vigneshwaran, S.; Sundarakannan, R.; John, K.M.; Deepak Joel Johnson, R.; Arun Prasath, K.; Ajith, S.; Arumugaprabu, V.; Uthayakumar, M. Recent advancement in the natural fiber polymer composites: A comprehensive review. *J. Clean. Prod.* **2020**, *277*, 124109. [CrossRef]
8. Yashas Gowda, T.G.; Sanjay, M.R.; Subrahmanya Bhat, K.; Madhu, P.; Senthamaraikannan, P.; Yogesha, B. Polymer matrix-natural fiber composites: An overview. *Cogent Eng.* **2018**, *5*, 1. [CrossRef]
9. Gon, D.; Das, K.; Paul, P.; Maity, S. Jute composites as wood substitute. *Int. J. Text. Sci.* **2012**, *1*, 84–93. [CrossRef]
10. Zakaria, M.; Ahmed, M.; Hoque, M.; Shaid, A. A Comparative Study of the Mechanical Properties of Jute Fiber and Yarn Reinforced Concrete Composites. *J. Nat. Fibers* **2020**, *17*, 676–687. [CrossRef]
11. Sinha, A.K.; Narang, H.K.; Bhattacharya, S. Mechanical properties of natural fibre polymer composites. *J. Polym. Eng.* **2017**, *37*, 879–895. [CrossRef]
12. Islam, M.M. Varietal Advances of Jute, Kenaf and Mesta Crops in Bangladesh: A Review. *Int. J. Bioorg. Chem.* **2019**, *4*, 24.
13. Rabbi, M.S.; Islam, T.; Bhuiya, M.M. Jute fiber reinforced polymer composite: A comprehensive review. *IJMPERD* **2020**, *10*, 3053–3072.
14. Zuhudi, N.Z.M.; Zulkifli, A.F.; Zulkifli, M.; Yahaya, A.N.A.; Nur, N.M.; Aris, K.D.M. Voids and Moisture Content of Fiber Reinforced Composites. *J. Adv. Res. Fluid Mech. Therm. Sci.* **2021**, *87*, 78–93. [CrossRef]
15. Rajendran Royan, N.R.; Leong, J.S.; Chan, W.N.; Tan, J.R.; Shamsuddin, Z.S.B. Current State and Challenges of Natural Fibre-Reinforced Polymer Composites as Feeder in FDM-Based 3D Printing. *Polymers* **2021**, *13*, 2289. [CrossRef]
16. Mohan, N.; Senthil, P.; Vinodh, S.; Jayanth, N. A review on composite materials and process parameters optimization for the fused deposition modelling process. *Virtual Phys. Prototyp.* **2017**, *12*, 47–59. [CrossRef]
17. Franco-Urquiza, E.A.; Escamilla, Y.R.; Llanas, P.I.A. Characterization of 3D Printing on Jute Fabrics. *Polymers* **2021**, *13*, 3202. [CrossRef]
18. Hinchcliffe, S.A.; Hess, K.M.; Srubar, W.V. Experimental and theoretical investigation of prestressed natural fiber-reinforced polylactic acid (PLA) composite materials. *Compos. B Eng.* **2016**, *95*, 346–354. [CrossRef]
19. Matsuzaki, R.; Ueda, M.; Namiki, M.; Jeong, T.-K.; Asahara, H.; Horiguchi, K. Three-dimensional printing of continuous-fiber composites by in-nozzle impregnation. *Sci. Rep.* **2016**, *6*, 23058. [CrossRef]
20. Mazzanti, V.; Malagutti, L.; Mollica, F. FDM 3D printing of polymers containing natural fillers: A review of their mechanical properties. *Polymers* **2019**, *11*, 1094. [CrossRef]
21. Mazzanti, V.; Mollic, F. In-process measurements of flow characteristics of wood plastic composites. *J. Polym. Environ.* **2017**, *25*, 1044–1050. [CrossRef]
22. Van den Oever, M.J.A.; Beck, B.; Müssig, J. Agrofibre reinforced poly (lactic acid) composites: Effect of moisture on degradation and mechanical properties. *Compos. A Appl. Sci. Manu.* **2010**, *41*, 1628–1635. [CrossRef]
23. Filgueira, D.; Holmen, S.; Melbø, J.K.; Moldes, D.; Echtermeyer, A.T.; Chinga-Carrasco, G. Enzymatic-assisted modification of thermomechanical pulp fibers to improve the interfacial adhesion with poly (lactic acid) for 3D printing. *ACS Sustain. Chem. Eng.* **2017**, *5*, 9338–9346. [CrossRef]
24. Osman, M.A.; Atia, M.R. Investigation of ABS-rice straw composite feedstock filament for FDM. *J. Rapid Prototyp.* **2018**, *24*, 1067–1075.
25. Sano, Y.; Matsuzaki, R.; Ueda, M.; Todoroki, A.; Hirano, Y. 3D printing of discontinuous and continuous fiber composites using stereolithography. *Addit. Manuf.* **2018**, *24*, 521–527.
26. Zhang, S.; Li, M.; Hao, N.; Ragauska, A.J. Stereolitography 3D printing of Lignin Reinforced Composites with Enhanced Mechanical Properties. *ACS Omega* **2019**, *4*, 20197–20204. [CrossRef]
27. Karalekas, D.E. Study of the mechanical properties of nonwoven fibre mat reinforced photopolymers used in rapid prototyping. *Mater. Des.* **2003**, *24*, 665–670. [CrossRef]
28. Ramírez-Hekrrera, C.A.; Cruz, I.C.; Jiménez-Cedeño, I.H.; Martínez-Romero, O.M.; Elías-Zúñiga, A. Influence of the Epoxy Resing Process Parameters on the Mechanical Properties of Produced Bidirectional Canbon/Epoxy Woven Composites. *Polymers* **2021**, *13*, 1273. [CrossRef]
29. Chen, J.; Lu, J.; Zhou, X. Adhesion properties of bio-based resins and their interaction with natural fibers in composite materials. *J. Compos. Mater.* **2021**, *55*, 1539–1550.
30. Zhang, W.; Yin, L.; Zhao, M.; Tan, Z.; Li, G. Rapid and non-destructive quality verification of epoxy resin product using ATR-FTIR spectroscopy coupled with chemometric methods. *Micromech. J.* **2021**, *168*, 106397. [CrossRef]

31. May, C.A. *Epoxy Resins: Chemistry and Technology*; Marcel Dekker, Inc.: New York, NY, USA, 1988; pp. 305–320.
32. Cecen, V.; Seki, Y.; Sarikanat, M.; Tavman, I.H. FTIR and SEM Analysis of Polyester- and Epoxy-Based Composites Manufactured by VARTM Process. *J. Appl. Polym. Sci.* **2008**, *108*, 2163–2170. [CrossRef]
33. Hong, C.K.; Hwang, I.; Kim, N.; Park, D.H.; Hwang, B.S.; Nah, C. Mechanical properties of silanized jute-polypropylene composites. *J. Industr. Eng. Chem.* **2008**, *14*, 71–76. [CrossRef]
34. Singh, A.A.; Palsule, S. Jute fiber reinforced chemically functionalized polypropylene self-compatibilizing composites by Palsule process. *J. Compos. Mater.* **2015**, *50*, 1199–1212. [CrossRef]
35. Wang, H.; Memon, H.; Hassan, E.A.M.; Miah, M.S.; Ali, M.A. Effect of jute fiber modification on mechanical properties of jute fiber composite. *Materials* **2019**, *12*, 1226. [CrossRef]
36. Gopinath, A.; Kumar, S.; Elayaperumal, A. Experimental investigations on mechanical properties of jute fiber reinforced composites with polyester and epoxy resin matrices. *Procedia Eng.* **2014**, *97*, 2052–2063. [CrossRef]
37. Ahamed, B.; Hasan, M.; Azim, A.Y.M.A.; Saifullarh, A.; Alimuzzaman, A.; Dhakal, H.N.; Sarker, F. High-performance short jute fiber preforms for thermoset composite applications. *Compos. Part C* **2022**, *9*, 100318.
38. Bledzki, A.K.; Jaszkiewicz, A. Mechanical performance of biocomposites based on PLA and PHBV reinforced with natural fibers-a comparative study to PP. *Compos. Sci. Technol.* **2010**, *70*, 1687–1696. [CrossRef]
39. Rahman, M.R.; Huque, M.M.; Islam, M.N.; Hasan, M. Improvement of physic-mechanical properties of jute fiber reinforced polypropylene composites by post-treatment. *Compos. A Appl. Sci. Manuf.* **2008**, *39*, 1739–1747. [CrossRef]
40. Huang, S.; Fu, Q.; Yan, L.; Kasal, B. Characterization of interfacial properties between fibre and polymer matrix in composite materials-A critical review. *J. Mater. Res. Technol.* **2021**, *13*, 1441–1484. [CrossRef]
41. Ambrosio, D.; Gabrion, X.; Malecot, P.; Amiot, P.; Thibaud, S. Influence of manufacturing parameters on the mechanical properties of projection sterolithography manufactured specimens. *Int. J. Adv. Manuf. Technol.* **2020**, *106*, 265–277. [CrossRef]
42. Chockalingam, K.; Jawahar, N.; Chandrasekhar, U. Influence of layer thickness on mechanical properties in stereolithography. *Rapid Prototyp. J.* **2006**, *12*, 106–113. [CrossRef]
43. Chockalingam, K.; Jawahar, N.; Chandrasekhar, U. Establishment of process model for part strength in stereolithography. *J. Mater. Process. Technol.* **2008**, *208*, 348–365. [CrossRef]
44. Dizon, J.R.C.; Espera, A.H., Jr.; Chen, Q.; Advincula, R.C. Mechanical characterization of 3D-printed polymers. *Addit. Manuf.* **2018**, *20*, 44–67. [CrossRef]